Available online at www.sciencedirect.com
ScienceDirect
IFAC PapersOnLine 52-14 (2019) 88–93

Control of Jet Flow Angle in Continuous Casting Process using an Electromagnetic Brake

Shereen Abouelazayem*. Ivan Glavinić,**
Thomas Wondrak*, Jaroslav Hlava******

** Technical University of Liberec, Studentská 1402/2, Liberec, Czech Republic (e-mail: shereen.abouelazayem@tul.cz)*
*** Helmholtz-Zentrum Dresden - Rossendorf, Bautzner Landstraße 400, Dresden, Germany (e-mail: i.glavinic@hzdr.de)*
**** Helmholtz-Zentrum Dresden - Rossendorf, Bautzner Landstraße 400, Dresden, Germany (e-mail: t.wondrak@hzdr.de)*
***** Technical University of Liberec, Studentská 1402/2, Liberec, Czech Republic (e-mail: jaroslav.hlava@tul.cz)*

Abstract: The flow pattern in the mould of the continuous casting is an important factor in determining the quality of the steel slabs that are produced in the end of the process. Hence it can heavily influence manufacturing costs due to the scrap percentage. Electromagnetic actuators are frequently used in the continuous casting process to stabilize the flow in the mould and therefore produce higher quality of steel slabs. Usually they are used in open loop but their effect on the flow pattern may be much better directed if they are used as a part of closed loop control based on real time measurements. In this paper, a closed loop controller is proposed that adjusts the magnetic field of an electromagnetic brake using the real time measurement of the angle of the jet flowing from the Submerged Entry Nozzle (SEN). The angle is kept within a specific range by the controller in order to prevent a deeper jet impingement into the mould; this allows us to achieve the desirable double roll flow pattern, and to avoid the entrapment of slug. The controller is based on a model of the relationship between brake current and jet angle that was obtained using experimental data from a laboratory scale continuous casting plant.

Keywords: Flow Control, Tomography, Process Automation, Model Predictive Control

1. INTRODUCTION

Continuous casting is very widely used in the industry both for steel and non-ferrous metals. Continuous casting process consists mainly of transforming the liquid metal to solid metal and the quality of the product obtained in the end of the process is heavily affected by many factors during this procedure. The process begins with the liquid metal flowing from a ladle to a 'tundish' which serves as a buffer vessel. The metal flows down through a Submerged Entry Nozzle (SEN) into a mould. The flow rate is there controlled by a stopper rod or a sliding gate. In the water cooled mould a thin solid shell on the metal surface is formed. The partly solidified strand is then continuously transported on rolls at a speed that matches the flow of the incoming metal and cooled by water sprays until it is solidified completely. This solidified strand can then be cut into slabs or billets and finally it can be removed from the plant without any interruption of the continuous process. (Thomas, 2003). Among the many factors that affect the quality of the final product, the molten metal level in the mould is especially important (Kitada, et al., 1998). This level should be as constant and flat as possible to provide a smooth shell formation and to avoid potential defects (Furtmueller & Re, 2008). This objective is not easily achieved because this control loop is affected by many disturbances like bulging, flow fluctuations and surface waves. Consequently, most of the published papers related to the continuous casting control have been focused on mould level control. The notion continuous casting control as used in the literature is mostly just another way to say mould level control. Somewhat less usually, the problem of temperature or temperature field control is also treated (see e.g. Belavý et al., 2015). However, despite its importance mould level is just a single variable. The objective that this level should be constant is not comprehensive enough to cover all quality requirements in the case of such complex process like continuous casting.

We propose going a step further and using sensors that are not limited to measuring one variable but can view what is happening inside the process. Particularly in the case of continuous casting mould, not just the liquid level but the whole flow pattern inside the mould is important. The optimum flow pattern observed in the mould is a symmetric double roll flow as opposed to the single roll (see Fig.1). The double roll flow allows for the impurities to rise to the free surface and as a result decreasing slug entrainment in the solid steel (Cukierski et al., 2007). Implementing flow pattern control in the mould has proven to be a challenge due to the unavailability of suitable sensors to provide information about the flow inside the mould. Continuous casting process operates in harsh conditions including extremely high temperatures due to the liquid steel, therefore eliminating the use of conventional sensors. Electromagnetic tomography provides a solution for the above issue, as it allows us to view the velocity fields inside the mould, and thus giving us an idea of the flow patterns inside.

10.1016/j.ifacol.2019.09.169

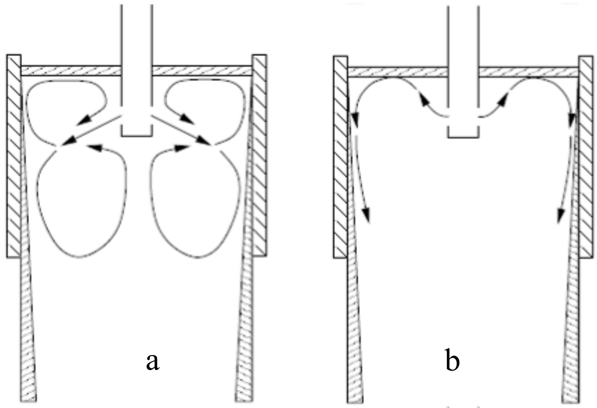

Figure 1: a) Double roll flow pattern, b) Single roll flow pattern

In this paper, we describe preliminary results of a research focused on this objective. The measured velocity fields in the mould are used to obtain the angle of the jet flow exiting from the SEN. In the end, the control objective will be to maintain the angle between the ranges of 10^o to 15^o to prevent deep jet impingement during the process. Therefore, avoiding the entrapment of slugs and sustaining the double roll flow. The actuator used to change this angle is the varying magnetic field of the electromagnetic brake (EMBr).

2. SYSTEM DESCRIPTION

2.1 Experimental Setup

The experiments described in this paper were conducted at the Mini-LIMMCAST facility in the Helmholtz-Zentrum Dresden-Rossendorf (HZDR), Dresden Germany. The Mini-LIMMCAST setup consists of a small-scale model of the continuous casting process for steel slabs (Timmel *et al*., 2010). The liquid steel is replaced with Gallium-Indium-Tin (GaInSn) alloy which is liquid at room temperature. The 'tundish' contains approximately 3.5 litres of GaInSn which is released into the glass mould through the SEN. The flow of the liquid is controlled by a stopper rod above the SEN. The focus of our experiments was on the flow patterns inside the mould. The position of the stopper rod was therefore kept constant during experiments to keep the flow into the mould constant. The liquid from the mould flows further into a storage vessel which is then pumped again into the 'tundish' in order to implement continuous experiments. This experimental device does not include the rollers with solidifying strand. As a result of it, most of the disturbances affecting the mould level control are not present and constant stopper rod position results in almost constant mould level.

2.2 Measurement system

Due to the opaqueness of the liquid, electromagnetic tomography sensors are needed to view the flow patterns inside of the mould. Contactless Inductive Flow Tomography (CIFT) has been successfully implemented on the Mini-LIMMCAST setup (Ratajczak *et al.,* 2016) and was used to reconstruct the velocity fields. The main concept of the CIFT technique relies on the flow of the conductive liquid going through a magnetic field created by the CIFT transmitter sensors. This creates electrical currents in the mould which results in an induced magnetic field. The induced magnetic field is measured by the receiver sensors and is used to reconstruct the velocity field in the mould.

This new flow measurement setup is currently being reconstructed for the updated experimental setup. For this reason, Ultrasonic Doppler Velocimetry (UDV) sensors are used as preliminary validation for the control of the angle of the exiting jet using EMBr in this study. The same control methodology will later be implemented with the CIFT and a comparison between the two sensor techniques will be implemented in order to validate the CIFT-based control loop.

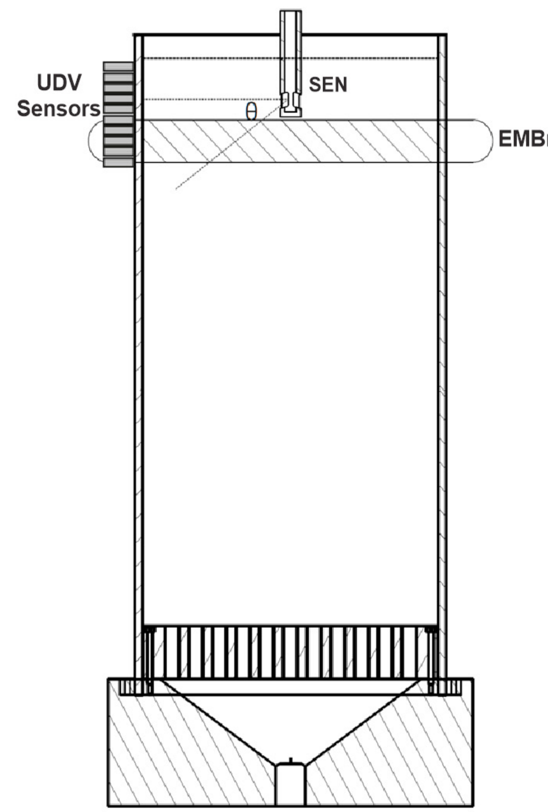

Figure 2: Mini-Limmcast Setup

As shown in Fig. 2, 10 UDV sensors are used to measure the horizontal velocities at the positions of the sensors. In our setup we will only concentrate on the left half of the region of the mould, and assume that there is symmetry between the two regions. The experiments conducted on the setup shows that the angle of the jet does not exceed beyond the horizontal level of the nozzle outlet, which we will consider as angle 0^o. Depending on the magnetic field from the brakes, the angle can vary from 0^o to 34^o. Due to the limitations of the movement of the angle, the sensors of interest are the lower 5 UDV sensors, in which their velocities will be used to track the oscillations of the jet. Fig. 3 shows the velocity measured by the fifth sensor from top. The velocities are measured at distance 70.4 mm from the mould wall. The figure shows that the signal needs to be smoothed as to find significant patterns in the data. A median filter is used to avoid smoothing out the fast transitions in velocity which are caused by the changes in the EMBr magnetic field.

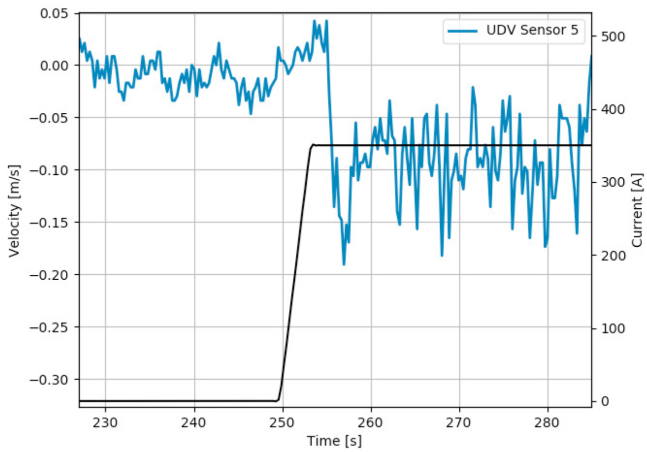

Figure 3: Dynamic velocity response to step increase in current from 0A to 350A

The direction of the velocity measured by the UDV sensors is identified by the sign of the velocity; negative velocities indicate that the flow is moving towards the sensors and mould wall, while positive velocities indicate that the flow is moving away from the sensors and mould wall (see Fig. 5). Cubic spline interpolation is used to provide a finer resolution between the lower 5 sensor positions. In order to track the movement of the jet, we need to compute the largest velocities with negative sign measured in the region surrounding the SEN outlet. During every frame captured by the sensors, the algorithm compares the interpolated velocities between the lower 5 sensors and computes the y-axis position of the most negative velocities. This is done for the majority of the points between the mould wall and the SEN; however, the algorithm avoids taking the velocities near the mould wall. The velocities too near to the mould wall are strongly fluctuating due to the high turbulence occurring from the jet hitting the wall of the mould. Therefore, these strongly fluctuating velocities are not considered when calculating the jet angle. After the most negative velocities have been computed, linear regression using least squares is used to fit a line that would represent the flow of the jet. The linear regression uses the quadratic loss function to calculate the error in the model (See Fig. 4). Fig. 5, 6 and 7 illustrate the reconstructed angle responses, and shows that the algorithm is able to track the movement of the jet sucessfully.

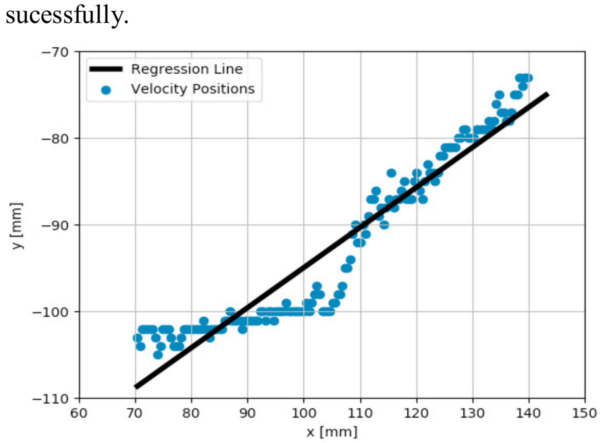

Figure 4: Linear regression line to fit positions of largest velocities with negative sign with EMBr turned off

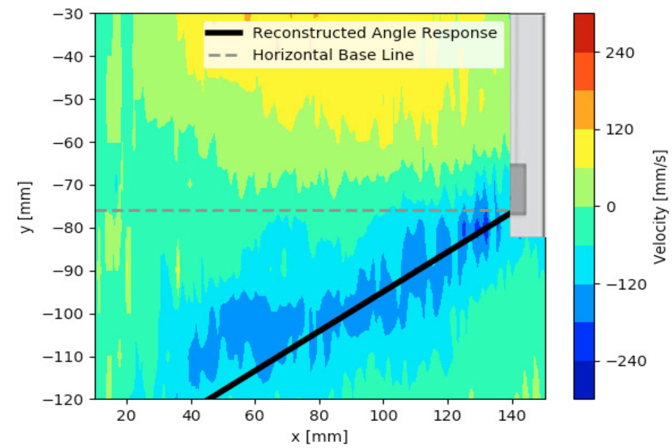

Figure 5: Reconstructed angle response with EMBr turned off

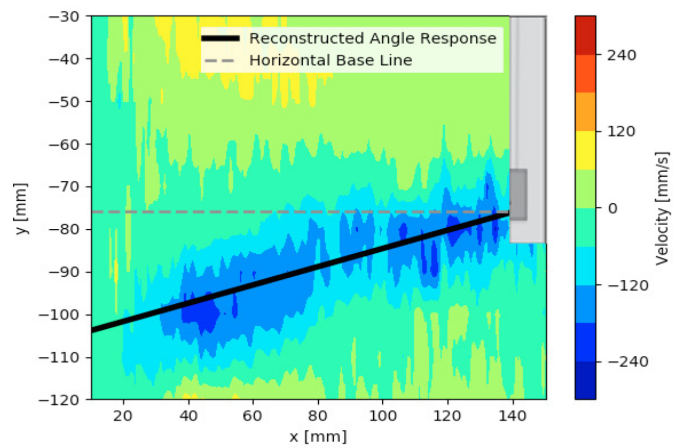

Figure 6: Reconstructed angle response with EMBr current of 250A

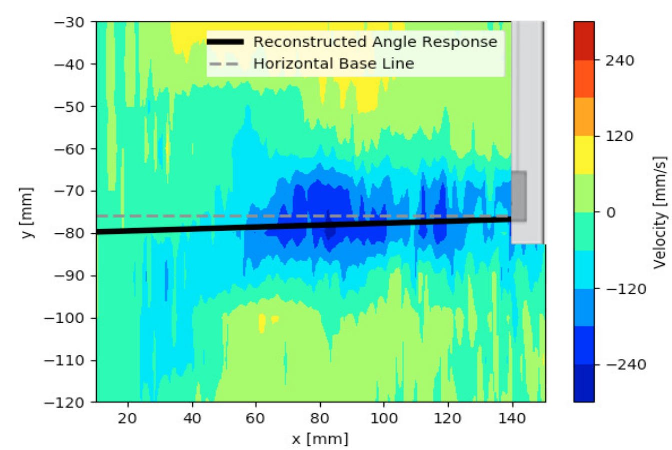

Figure 7: Reconstructed angle response with EMBr current of 450A

2.3 *Electromagnetic Brakes (EMBr)*

The main actuator in the proposed control loop is the electromagnetic brake. Electromagnetic actuation is commonly used to stabilize the turbulent flow in the mould. The electromagnetic forces applied can either be static (electromagnetic brakes) or rotating (electromagnetic stirrers). What is however much less common is the use of electromagnetic actuators for the closed loop control.

One of the few attempts is described in (Dekemele *et al.*, 2016). In this paper an electromagnetic stirrer was used to both brake and accelerate the liquid steel flow in the mould in order to keep the flow speed at an optimal range. A sensor was used for the drag force to measure the flow at a certain point in the mould. The controller (both PI and MPC were tested) was based on model identified from the experimental data. The use of the closed loop controlled electromagnetic actuation proposed in the present paper is different from the previous attempts described in the literature. In our setup a static electromagnetic field is applied by the EMBr with the objective to control the flow pattern. The static electromagnetic field produced by the EMBr induces current in the conducting liquid, which generates a force that opposes the flow (Chaudhary *et al.*, 2012). As shown in Fig. 8, a wide "single ruler" EMBr is used to apply the magnetic field. The ruler is placed right below the outlet of the SEN instead of directly at the outlet level. It has been shown that this position for the brakes is better for stabilizing the jet flow (Thomas & Cho, 2018).

By analysing the flow in the mould during the experiments, it becomes clear that due to the "braking effect" caused the magnetic field below the SEN outlet; the exiting jet becomes more horizontal. In Fig. 7 the exiting jet approaches the horizontal base line. The EMBr is controlled by varying the current going to the coils which results in variations to the magnetic field applied on the conductive liquid in the mould. These experiments were conducted on the Mini-LIMMCAST setup while the UDV sensors recorded the velocity fields in the mould.

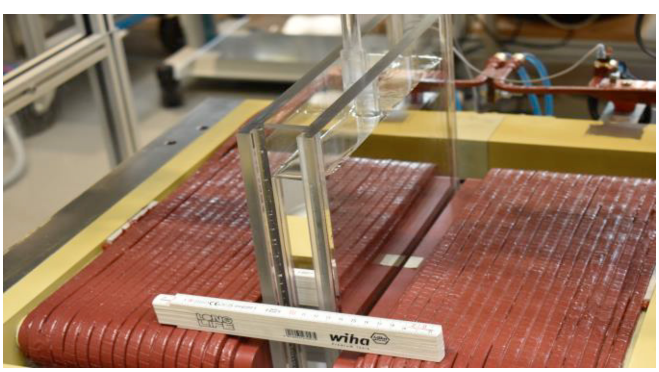

Figure 8: Electromagnetic Brakes (EMBr) in Mini-LIMMCAST setup

3. CONTROL LOOP

3.1 Model Description

A model for the system was created using the System Identification Toolbox in MATLAB; specifically process model estimation was used to create the transfer function describing the linear system dynamics. Different models can be created by varying the number of poles and zeros. Also integrators and time delays can be added to create the transfer function. It turned out that the relationship between brake current and jet angle can be described by a linear model in the form of the following first order model.

$$G(s) = \frac{-0.04429}{1.4443s+1} \tag{1}$$

Furthermore, second and third order models were created and their performance were compared as shown in Table 1.

Model	Fit Percent
1st Order Model	80.4%
2nd Order Model	82.2%
3rd Order Model	78.1%

Table 1: Performance Comparison using Fit Percentage

Fit percent represents the normalized root mean squared error:

$$Fit\ Percent = 100\left(1 - \frac{\|y_{measured} - y_{model}\|}{\|y_{measured} - \bar{y}_{measured}\|}\right) \tag{2}$$

Although the second order model slightly outperforms the first order model, there should be a trade-off between the complexity of the model and its accuracy. In the end, the added complexity of the second order model does not improve the fit percentage significantly, which is why the first order model was selected. Comparison of the first order model output with measurement (where the angle was calculated from the UDV data using the procedure described above) is shown in Fig. 9. This figure gives the response to a series of random step changes of the EMBr current. It can be observed that there is a good fit between this first order model and measured data. Fast dynamics and relatively short time constant of model (1) are due to the rapid responses of the velocity fields in the region of interest to the changes in the magnetic field produced by the brakes.

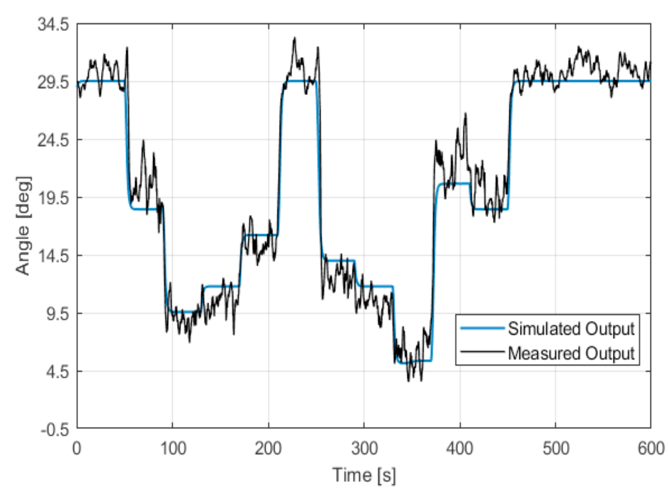

Figure 9: Comparison of simulated model output with measured output

3.2 Model Predictive Control (MPC)

The objective of the controller is to maintain the jet angle in the range between 10º and 15º during the operation of the casting process. Additionally, there are constraints on the input current to the electromagnetic brake. Due to the above reasons a controller based on Model Predictive Control was used in the control loop. MPC is known to outperform PID both in constraint handling and range control. The Model Predictive Control Toolbox in MATLAB was utilized for this step. The algorithm begins by converting the first order model into the below discrete time state space form:

$$x_p(k+1) = A_p x_p(k) + BS_i u_p(k) \tag{3}$$

$$y_p(k) = {S_o}^{-1} C x_p(k) + {S_o}^{-1} D S_i u_p(k) \tag{4}$$

Where A_p, B, C, D are the state-space matrices. S_i and S_o are the input and output scale factors. x_p is the state vector. u_p is the input variables. y_p is the output variables. A quadratic cost function is used for the optimization problem in order to determine the manipulated variable that should be applied in the future.

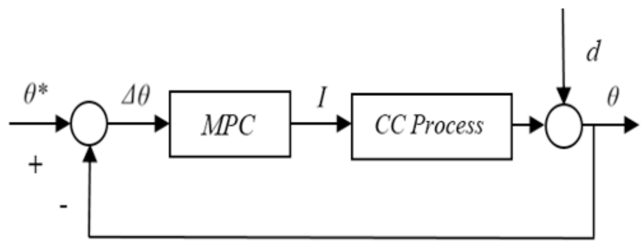

Figure 10: Closed control loop for CC

The most important disturbance affecting the control loop is the nozzle clogging. This clogging is a serious issue when it comes to the quality of the steel slabs as it can cause asymmetric and unstable flow in the mould (Thomas, 2018). In one of our simulations we introduce nozzle clogging as a disturbance to our process so that we can assess how efficiently the controller is able to maintain the optimum angle range, while rejecting the disturbance produced by the nozzle clogging. We assumed that the clogging is occurring on the opposite side of the nozzle. Due to the blocked area on the one side of the nozzle, the flow exiting the opposite outlet is increased, which results in a deeper jet impingement in the mould as shown in (Cho et al., 2012).

The clogging disturbance *d* (see Fig. 10) can be modelled as output disturbance because it directly changes the angle of the jet (Cho et al., 2012). The clogging and unclogging have different dynamics. Clogging of the nozzle occurs gradually with time; therefore, a ramp function should be used to simulate the increase in jet angle. However, unclogging may be much faster. Typically, pieces of the clogged material break off into the flow in the mould and the effect is quite sudden. This can adequately be modelled as step disturbance. Both clogging and unclogging were simulated to see how the controller reacts to both situations.

4. RESULTS

4.1 Simulation experiments

Two sets of simulations were implemented; the first simulation included set point tracking where we analysed the controller's response to various changes to the set point (see Fig. 11 and 12), four different set points were used at intervals of t=20s for this simulation. The controller was able to successfully track the set point with an average settling time of t=5s. The second set of simulations concentrated on disturbance rejection (see Fig.13 and 14) which is the main concentration of this study. Disturbance due to clogging was introduced at t=20s which resulted in a gradual increase in the angle response. Furthermore, the effect of unclogging was also introduced at t=50s which decreased the angle response. In both the clogging and unclogging disturbances, the MPC was able to respond quickly and reject the disturbances in order to maintain the set point reference. We avoided using a more aggressive control effort by the MPC as to avoid reaching saturation in the input control. Furthermore, we implemented open loop control which is generally used in industry, and compared it with our design for the closed loop control; Fig. 13 shows a closed loop system is needed to prevent the angle from rapidly increasing, and therefore avoid a deeper jet impingement into the mould due to disturbances such as nozzle clogging.

4.2 SEN Clogging Detection

An interesting characteristic that was observed during the simulations was the control effort needed to reject the disturbance and maintain the optimum angle range. Fig. 14 shows that during the disturbance that occurs at t=20s, the current needed to keep the angle in the optimum range is continuously increasing. This observation can be utilised for fault detection in the continuous casting process; where by using the input current to the EMBr, we can detect the rate of clogging in the SEN. Normally during the casting process, detection of nozzle clogging is a challenge due to the harsh conditions of the process itself. By observing the rate of current of the EMBr in the closed loop control implemented in this study, we can have more information about the clogging that occurs in the SEN. For future work, it would be interesting to expand the closed loop by implementing argon gas injection as another actuator that would utilise the information about the clogging from the input current to the EMBr.

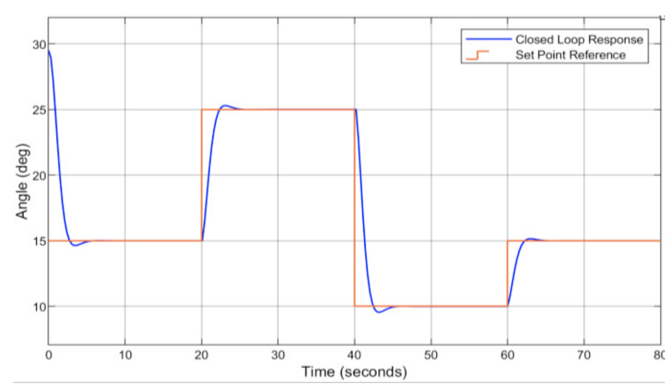

Figure 11: Closed loop response for set point tracking

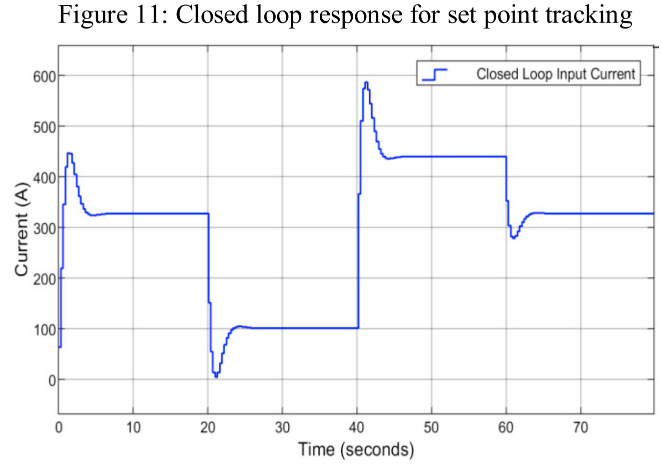

Figure 12: Input current for set point tracking

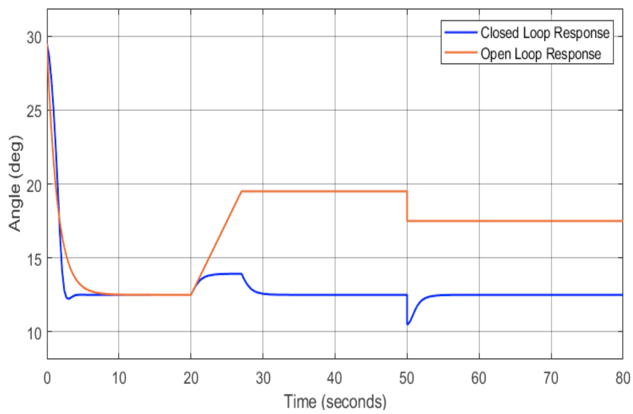

Figure 13: Comparison of angle responses for disturbance rejection: closed loop vs open loop configuration

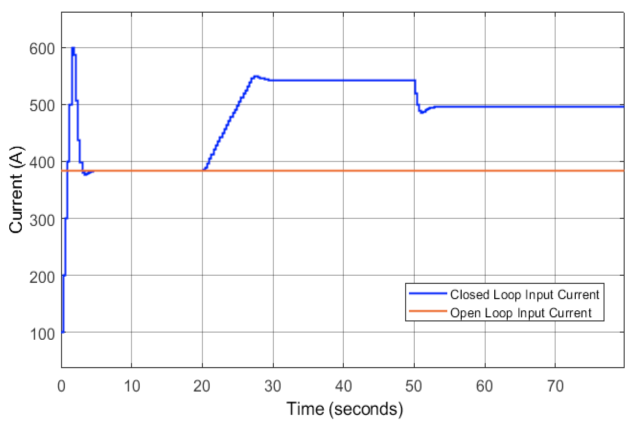

Figure 14: Comparison of brake current during disturbance rejection: closed loop vs open loop configuration

5. CONCLUSION

In this paper we have demonstrated that by using the velocity fields measured by the UDV we are able to analyse the flow patterns in the mould, specifically the behaviour of the jet exiting the SEN. The study showed that a control loop based on MPC is able to sufficiently control the angle of the jet and keep it within the optimum range, therefore controlling the flow pattern in the mould. The simulations included the clogging and unclogging of the SEN as disturbances to the process in order to assess the disturbance rejection of the controller. In the end, it was shown that the proposed controller is able to maintain the optimum angle range even with the disturbances introduced. Furthermore, it was shown that the rate of current of the EMBr in the closed loop control can indicate clogging in the SEN. In the end, by validating the concept of using velocity fields in the mould to control the flow patterns, the concept will be extended to using tomographic sensors, specifically CIFT sensors which can be implemented in the harsh conditions of a real caster. Similar control techniques will be used with the CIFT sensors and the results will be validated with the results from the UDV sensors.

ACKNOWLEDGMENTS

This work has received funding from the European Union's Horizon 2020 research and innovation program under the Marie Skłodowska-Curie grant agreement No 764902. (TOMOCON - www.tomocon.eu)

REFERENCES

Belavý, C., G. Hulkó, L. Bartalský, and M. Kubiš (2015), "Robust Control of Temperature Fields in Steel Casting Mould as Distributed Parameter Systems." IFAC-PapersOnLine, 8th IFAC Symposium on Robust Control Design ROCOND 2015, 48 (14): 408–13.

Chaudhary, R., Thomas, B. G., & Vanka, S. P. (2012). Effect of Electromagnetic Ruler Braking (EMBr) on Transient Turbulent Flow in Continuous Slab Casting using Large Eddy Simulations. Metallurgical and Materials Transactions B, 43(3), 532–553.

Cho, S.-M. et al. (2012) 'Effect of nozzle clogging on surface flow and vortex formation in the continuous casting mold', Iron and Steel Technology, 9, pp. 85–95.

Cukierski, K. and Thomas, B. G. (2008) 'Flow Control with Local Electromagnetic Braking in Continuous Casting of Steel Slabs', Metallurgical and Materials Transactions B, 39(1), pp. 94–107.

Dekemele, K., Ionescu, C., Doncker M. De and De Keyser, R. (2016), Closed loop control of an electromagnetic stirrer in the continuous casting process, 2016 European Control Conference (ECC), Aalborg, 2016, pp. 61-66.

Furtmueller, C., and L. del Re. (2008), "Control Issues in Continuous Casting of Steel." IFAC Proceedings Volumes 41 (2): 700–705.

Kitada, H., Kondo, O., Kusachi, H. and Sasame, K. (1998), "H infinity Control of Molten Steel Level in Continuous Caster," IEEE TRANSACTIONS ON CONTROL SYSTEMS TECHNOLOGY, vol. 6, no. 2, p. 8, 1998.

Ratajczak, M. et al. (2016) 'Contactless inductive flow tomography: recent developments in its application to continuous casting with electromagnetic brakes', p. 8.

Thomas, B. G. (2003) 'On-line Detection of Quality Problems in Continuous Casting of Steel', p. 16.

Thomas, B. G., and S. M. Cho (2018), Overview of Electromagnetic Forces to Control Flow During Continuous Casting of Steel, IOP Conference Series: Materials Science and Engineering 424 (October): 012027.

Thomas, B. G. (2018) 'Review on Modeling and Simulation of Continuous Casting', steel research international, 89(1), p. 1700312.

Timmel, K., Eckert, S., Gerbeth, G., Stefani, F., & Wondrak, T. (2010). Experimental Modeling of the Continuous Casting Process of Steel Using Low Melting Point Metal Alloys—the LIMMCAST Program. ISIJ International, 50(8), 1134–1141.